Research Article | Vol. 25, No. 19 | 18 Sep 2017 | OPTICS EXPRESS 22455
Optics EXPRESS

Miniaturized compound refractive X-ray zoom lens

E. KORNEMANN,[1,*] O. MÁRKUS,[1] A. OPOLKA,[1] T. ZHOU,[2] I. GREVING,[3] M. STORM,[4] C. KRYWKA,[3] A. LAST,[1] AND J. MOHR[1]

[1]*Institute of Microstructure Technology (IMT), Karlsruhe Institute of Technology (KIT), Hermann-von-Helmholtz-Platz 1, 76344 Eggenstein-Leopoldshafen, Germany*
[2]*ESRF - The European Synchrotron Radiation Facility, 71 Avenue des Martyrs, 38043 Grenoble, France*
[3]*Institute of Materials Research, Helmholtz-Zentrum Geesthacht, Max-Plank-Str. 1, 21502 Geesthacht, Germany*
[4]*Diamond Light Source Ltd, Didcot, Oxfordshire OX11 0DE, UK*
**elisa.kornemann@kit.edu*

Abstract: We introduce the concept of a miniaturized compound refractive X-ray zoom lens consisting of SU-8 lenses fabricated by deep X-ray lithography. The focal length can be varied by changing the number of lens elements placed in the beam. We use suitable actuators to move single lens elements reversibly out of the beam. The X-ray zoom lens can accept different X-ray energies while keeping a fixed working distance, or vary the focal distance for a fixed energy. The latter is useful in tuning the magnification factor in full field microscopy.

OCIS codes: (340.0340) X-ray optics; (340.7440) X-ray imaging; (340.7460) X-ray microscopy; (110.7440) X-ray imaging; (300.6560) Spectroscopy, x-ray; (080.3620) Lens system design.

References and links

1. T. Tomie, "X-ray lens," Japanese patent 6–045288 (February 18, 1994), U.S. patents 5,594,773 (January 14, 1997) and 5,684,852 (1997).
2. A. Snigirev, V. Kohn, I. Snigireva, and B. Lengeler, "A compound refractive lens for focusing high-energy X-rays," Nature **384**(6604), 49–51 (1996).
3. B. Lengeler, C. G. Schroer, M. Kuhlmann, B. Benner, T. F. Gunzler, O. Kurapova, A. Somogyi, A. Snigirev, and I. Snigireva, "Beryllium parabolic refractive X-ray lenses," AIP Conf. Proc. **705**, 748–751 (2004).
4. B. Lengeler, C. G. Schroer, B. Benner, A. Gerhardus, T. F. Günzler, M. Kuhlmann, J. Meyer, and C. Zimprich, "Parabolic refractive X-ray lenses," J. Synchrotron Radiat. **9**(3), 119–124 (2002).
5. A. Stein, K. Evans-Lutterodt, N. Bozovic, and A. Taylor, "Fabrication of silicon kinoform lenses for hard x-ray focusing by electron beam lithography and deep reactive ion etching," J. Vac. Sci. Technol. B **26**(1), 122–127 (2008).
6. B. Nhammer, C. David, H. Rothuizen, J. Hoszowska, and A. Simionovici, "Deep reactive ion etching of silicon and diamond for the fabrication of planar refractive hard x-ray lenses," Microelectron. Eng. **67–68**, 453–460 (2003).
7. Y. Ohishi, A. Q. R. Baron, M. Ishii, T. Ishikawa, and O. Shimomura, "Refractive x-ray lens for high pressure experiments at SPring-8," Nucl. Instrum. Methods Phys. Res. A **467–468**, 962–965 (2001).
8. F. Marschall, A. Last, M. Simon, M. Kluge, V. Nazmov, H. Vogt, M. Ogurreck, I. Greving, and J. Mohr, "X-ray full field microscopy at 30 keV," J. Phys. Conf. Ser. **499**, 012007 (2014).
9. E. Reznikova, T. Weitkamp, V. Nazmov, M. Simon, A. Last, and V. Saile, "Transmission hard x-ray microscope with increased view field using planar refractive objectives and condensers made of SU-8 polymer," J. Phys. Conf. Ser. **186**, 012070 (2009).
10. V. Nazmov, E. Reznikova, A. Last, J. Mohr, V. Saile, M. DiMichiel, and J. Göttert, "Crossed planar x-ray lenses made from nickel for x-ray micro focusing and imaging applications," Nucl. Instrum. Methods Phys. Res. A **582**(1), 120–122 (2007).
11. A. Snigirev, I. Snigireva, G. Vaughan, J. Wright, M. Rossat, A. Bytchkov, and C. Curfs, "High energy x-ray transfocator based on Al parabolic refractive lenses for focusing and collimation," J. Phys. Conf. Ser. **186**, 012073 (2009).
12. H. Simons, F. Stöhr, J. Michael-Lindhard, F. Jensen, O. Hansen, C. Detlefs, and H. Friis Poulsen, "Full-field hard x-ray microscopy with interdigitated silicon lenses," Opt. Commun. **359**, 460–464 (2016).
13. C. G. Schroer and B. Lengeler, "Focusing hard x rays to nanometer dimensions by adiabatically focusing lenses," Phys. Rev. Lett. **94**(5), 054802 (2005).

#297583 https://doi.org/10.1364/OE.25.022455
Journal © 2017 Received 9 Jun 2017; revised 17 Aug 2017; accepted 25 Aug 2017; published 7 Sep 2017

Optics EXPRESS

14. F. Marschall, *Entwicklung Eines Röntgenmikroskops für Photonenenergien von 15 keV bis 30 keV* (KIT Scientific Publishing, 2014).
15. G. B. M. Vaughan, J. P. Wright, A. Bytchkov, M. Rossat, H. Gleyzolle, I. Snigireva, and A. Snigirev, "X-ray transfocators: focusing devices based on compound refractive lenses," J. Synchrotron Radiat. **18**(Pt 2), 125–133 (2011).
16. G. M. A. Duller, "F-Switch: Novel Random Access Manipulator for Large Numbers of Compound Refractive Lenses," MEDSI 2016 Conf Proc WEPE22 (to be published).
17. V. Nazmov, E. Reznikova, J. Mohr, A. Snigirev, I. Snigireva, S. Achenbach, and V. Saile, "Fabrication and preliminary testing of X-ray lenses in thick SU-8 resist layers," Microsyst. Technol. **10**(10), 716–721 (2004).
18. A. Snigirev, I. Snigireva, M. Drakopoulos, V. Nazmo, E. Reznikova, S. Kuznetsov, M. Grigoriev, J. Mohr, and V. Saile, "Focusing properties of X-ray polymer refractive lenses from SU-8 resist layer," Proc. SPIE **5195**, 21 (2003).
19. V. G. Kohn, I. Snigireva, and A. Snigirev, "Diffraction theory of imaging with X-ray compound refractive lens," Opt. Commun. **216**(4-6), 247–260 (2003).
20. V. G. Kohn, "An Exact Theory of Imaging with a Parabolic Continuously Refractive X-ray Lens," J. Exp. Theor. Phys. **97**(1), 204–215 (2003).
21. E. Gullikson, "Index of refraction," http://henke.lbl.gov/optical_constants/getdb2.html
22. S. G. Lipson, D. S. Tannhauser, and H. S. Lipson, *Optical Physics*, 3rd edition (Cambridge University, 1995).

1. Introduction

Compound Refractive X-ray Lenses (CRLs) are well established optics for hard X-rays for photon energies above about 10 keV. They consist of a large number of focusing lens elements, first described in [1, 2]. Today, they are fabricated from beryllium [3], aluminum [4], silicon [5], diamond [6], photoresist [7–9] or other materials. The most common type of CRL consists of many identical, biconcave, parabolic lens elements, aligned along the optical axis and is used in many applications [8–12]. In some applications the geometry of the individual lens elements is varied, such as in the case of adiabatic lenses [13]. Variable aperture CRLs have been described for full field microscopy with increased field of view [8, 14].

So called transfocators have been designed to tune the focal length [15]. In these transfocators sets of 2n CRL elements can be removed using pneumatic actuators. Most commonly transfocators are based on embossed rotational symmetric Be-CRLs with focal lengths in the meter range. The F-Switch is a more advanced device with 120 randomly selectable point focusing CRLs [16]. In this F-Switch two stepper motors drive a switching claw along a lead-screw. The claw pushes a lens element out of the beam via an actuation blade. When the blade is pulled back, a spring pushes the lens element back into the beam. Bistable springs hold the elements in position. In addition to the transfocator the effective center of the lens can be translated along the beam direction and thus finer control of the position of the focal plane is possible. The F-Switch normally operates in an energy range of 6-18 keV and provides focal spot sizes of 5-100 µm. A typical change in lens configuration is performed in about 30 s. All these devices with changeable focal length are used for beam conditioning.

In this paper we present a new X-ray zoom lens for imaging e.g. in full field microscopy which is based on CRLs made from SU-8 resist by deep X-ray lithography. The zoom lens has an overall volume of only about two liters [see Fig. 8]. It uses piezo actuators to move individual lens elements in and out of the beam. Due to its compactness it can be easily included in different experimental setups. The adjustment of the focal length of the zoom lens can be controlled remotely within fractions of a second to fit a new source or sample distance or to choose another magnification ratio. Additionally, if the same sample shall be examined with different energies in the same setup, the software of the zoom lens controller will calculate the necessary focal length and the best lens configuration will be set automatically. The zoom lens can be configured for line or point focus, or even astigmatic geometry to compensate for asymmetrical source dimensions, and thereby achieve a more roundish focal spot on a sample.

Optics EXPRESS

2. The rationale and optical design

At KIT/IMT refractive X-ray lenses are produced from the highly-sensitive negative resist SU-8 which shows high X-ray transparency [17]. The SU-8 polymer resist, which is cross-linked during initial X-ray exposure (fabrication), is not significantly modified by later X-ray exposures when using a lens. This type of CRLs have been proven to be long time radiation stable at different synchrotron radiation applications up to a deposited dose of at least 2 MJ/cm3 [17, 18]. Hundreds of well aligned, refractive lens elements with radii of curvature in the range of a few micrometers can be made in a single step via deep X-ray lithography. The geometry of the structures is defined during electron beam writing of the X-ray absorber mask mandatory for X-ray lithography.

The focal length f of a CRL made of equidistant and identical elements with total length L, radius of curvature in the apex of the parabola R and N lens elements is approximated by [19, 20]

$$f = \frac{R}{2\delta N} + \frac{L}{6}. \tag{1}$$

For X-rays the complex refractive index n of any material is slightly below one and commonly written as

$$n = 1 - \delta + i\beta. \tag{2}$$

with β being the absorption coefficient and δ the decrement of the refractive index. For SU-8 resist (type "mr-X-50" from micro resist technology GmbH, Berlin) we measured δ for photon energies E, in the range of 8.7 keV to 40 keV. The values can be approximated by

$$\delta = \frac{0.00027142 / keV^2}{(E / keV)^2}. \tag{3}$$

For the absorption coefficient β we used data given in literature [21]. Usually several parallel CRLs are processed on one substrate. Due to the lithographic processing these are 1D refractive lenses producing a line focus. When a 2D-lens with a point focus is required two line focus lenses are combined and mounted into each other, with one of them rotated by 90° with respect to the other around the optical axis [see Fig. 1].

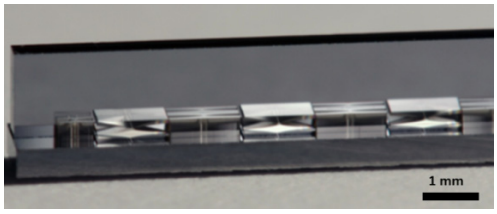

Fig. 1. Two SU-8-lens halves mounted with one half rotated by 90° with respect to the other around the optical axis for point focus imaging.

A zoom lens demands the possibility of varing the number of lens elements N. Therefore, the silicon substrates carrying the line focus CRLs are sawn into separate stripes [see Fig. 2]. They can be bent reversibly in and out of the beam with suitable piezo bender actuators.

Optics EXPRESS

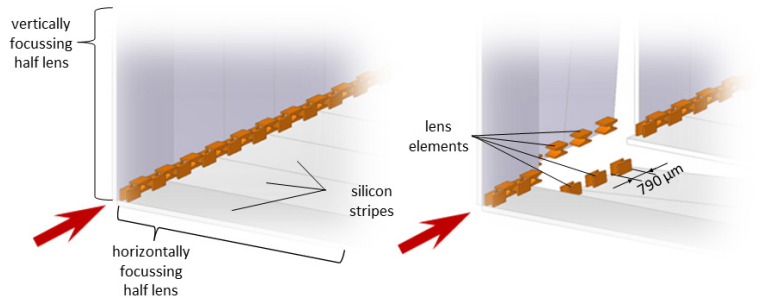

Fig. 2. Principle of an X-ray zoom lens made out of SU-8 CRLs from KIT/IMT with all lens elements in the beam (right) and four elements of each half lens bent out of the beam (left); one lens element is 790 µm long.

A pre-existing layout for fabricating the CRL (KIT/IMT layout number 1405_00_A0, #10) was used to build up the prototype version of the zoom lens. With its equally sized and comparatively large lens elements it is convenient for proving the principle and realization of a first miniaturized X-ray zoom lens. The CRL parameters are: aperture A = 250 µm; Nmax = 36 per half lens; radius of curvature R = 20 µm and air gap between two elements of 20 µm. The vertically focusing half lens is separated in 18 silicon stripes (v01 - v18) while the horizontally focusing half lens has been cut in 19 silicon stripes (h01 - h19). Each silicon stripe carries one or two lens elements. The exact composition is shown in Fig. 3.

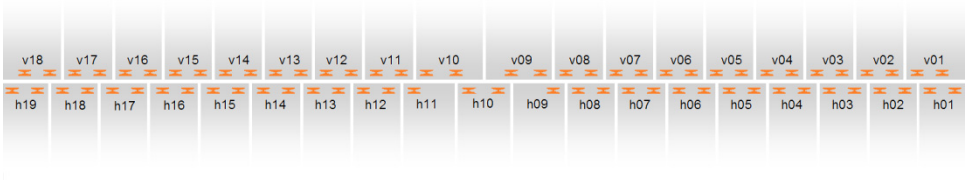

Fig. 3. CRL-layout 1405_00_A0, #10 of the two half lenses dedicated to the bendable vertically focusing (v01 - v18) and horizontally focusing (h01 - h19) silicon stripes.

With this CRL-layout the X-ray zoom lens can handle energies from 8 keV to 30 keV and provide focal lengths from the millimeter to meter range. Figure 4 presents a numerical example of the tunability of the zoom lens with a chosen sample distance d_s from sample to entrance aperture of the zoom lens of d_s = 1 m and four exemplary image distance d_i from entrance aperture of the zoom lens to the detector and resulting magnification factors of M = 2, 5, 10 and 20. The graph shows the selectable zoom lens configuration (from inserting 2 up to 36 lens elements in the beam) for different photon energies E.

Optics EXPRESS

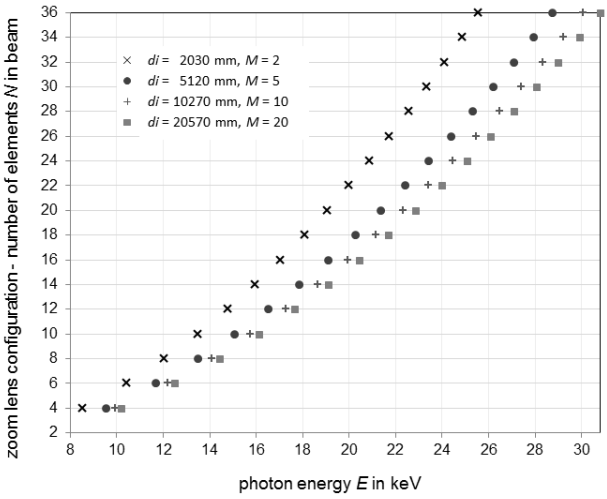

Fig. 4. Tunability of the X-ray zoom lens with the CRL-layout 1405_00_A0, #10 for a sample distance d_s of 1 m and exemplary chosen four image distances d_i with resulting magnification factor M. The zoom lens configuration is given as a function of the energy with number of elements N by each step switching off one actuator from source side to detector side.

Here, only the simplest case of switching one actuator and adding each time two lens elements in the beam is shown (18 out of 262143 lens configurations). For a number of switched actuators k (elements in beam: $N = 2k$) and total number of available actuators n ($n = 18$ for this zoom lens example) a certain number of different photon energies N_{Ph} can be selected, because the position of the lens element is important even when all elements are identical:

$$N_{\mathrm{Ph}} = \sum_{k=1}^{n} \binom{n}{k} = 2^n - 1. \tag{4}$$

When all lens elements are in the beam, the calculated transmission of the CRL increases with rising energy from 3% at 8 keV to 47% at 30 keV, then at 30.5 keV dropping to 23% due to an absorption edge of the lens material and again rising to 47% at 50 keV.

The achievable minimum focal spot size is determined by contributions from the size of the demagnified image of the source $\sigma_{\mathrm{min.phys}}$, from diffraction due to a limited lens aperture $\sigma_{\mathrm{min.diff}}$ and from the astigmatism $\sigma_{\mathrm{min.astigmatic}}$. The image size of the source $\sigma_{\mathrm{min.phys}}$ (FWHM) is calculated using the following equation

$$\sigma_{\mathrm{min.phys}} = \frac{d_i h_o}{d_o} \tag{5}$$

with d_i being the image distance, d_o the source distance and h_o the source size (FWHM). There can be a difference in the horizontal and vertical direction. For a source size $h_o = 100$ µm in $d_o = 50$ m distance, a photon energy of $E = 10$ keV and focal length of $f = 113$ mm the minimum focal spot size is calculated to $\sigma_{\mathrm{min.phys}} = 0.23$ µm. The contribution of the diffraction limit to the focal spot size is dependent on the wavelength λ and the numerical aperture NA by [22]

$$\sigma_{\mathrm{min.diff}} = \frac{\lambda}{NA}. \tag{6}$$

In the above mentioned example diffraction limits the minimum focal spot size to $\sigma_{\mathrm{min.\ diff}} = 0.25$ µm.

Optics EXPRESS

As displayed in Fig. 3, the lengths of the horizontally and vertically focussing lenses are not equal. Therefore, the lens is slightly astigmatic. In each symmetric mode, where always a pair of horizontal and vertical lens elements are bend out of the beam (e.g. v01, h01), the lens length differs by ΔL = 1615 µm, which is the length of two lens elements plus two air gaps. This results in an astigmatic lens with different focal length in the tangential and in the sagittal plane of Δf = 1158 µm at a photon energy of E = 10 keV with focal length f = 113 mm. In the center between these focal planes the diameter of the beam $\sigma_{\text{min. astigmatic}}$ (FWHM) is

$$\sigma_{\text{min.astigmatic}} = \frac{A_{\text{eff}}\Delta f}{2f} \tag{7}$$

with the effective aperture A_{eff}. The effective aperture A_{eff} is defined as the aperture limited by rays with a minimum transmission of 10% of the maximum transmission. In the example above $\sigma_{\text{min.astigmatic}}$ is calculated to be 0.28 µm.

3. Mechanical design and construction

We have chosen piezo bender actuators (type BA4902 from PiezoDrive, Newcastle, Australia) to move single lens elements reversibly in and out of the beam. This is because although they are small in dimensions (width 2 mm, thickness 0.75 mm, length 49 mm) they can still exert sufficient force (0.1 N) to bend the silicon stripes up to 400 µm at its free end, as required for moving the lens elements out of the beam.

Figure 4 schematically shows how the piezo bender actuators are clamped to the silicon stripes. These stripes are in mechanical contact with a deadlock bar aligning all stripes by slightly pre-stressing them. If a piezo bender actuator is switched off, the corresponding silicon stripe is not in mechanical contact with the actuator. Acting as a leaf spring, each stripe then returns to its initial position, positioning the lens elements in the beam. Together with the connecting cross-bar all bending stripes form solid state hinges [see Fig. 5], ensuring extremely accurate repositioning when actuating the stripes. The accuracy of the lens element positioning is thus only limited by the geometry of the deadlock bar. If the actuator is switched on, it bends the silicon stripe down with the deflection Δz describing the achieved movement of the CRL at the free end of the silicon stripe.

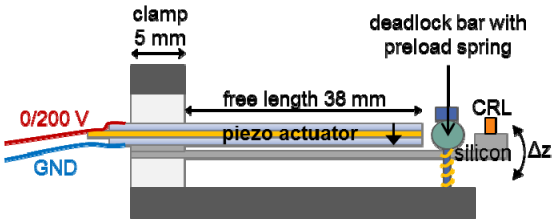

Fig. 5. Actuation principle of an X-ray zoom lens with piezo bender actuator on silicon stripes holding the CRL elements.

In order to build a zoom lens, a 400 µm thick SU-8 resist on a 525 µm thick silicon substrate is exposed with a mask providing several lens rows and then developed. The substrate is separated into individual line focus CRL rows by cutting with a wafer saw. Subsequently, one CRL is selected for the zoom lens and this CRL is glued out of center onto a 380 µm Si-wafer. This Si-wafer is put onto an adhesive carrier foil and cut perpendicular to the optical axis of the CRL into single silicon stripes [see Fig. 3]. The cuts are positioned in between two pairs of two lens elements. The relative position of the stripes remains unchanged in the cutting step. To connect these silicon stripes of the CRL at the opposite end a 5 mm x 60 mm Si-bar is glued parallel to the optical axis of the CRL onto the Si-wafer before it is taken off from the carrier foil [see Fig. 6].

Optics EXPRESS

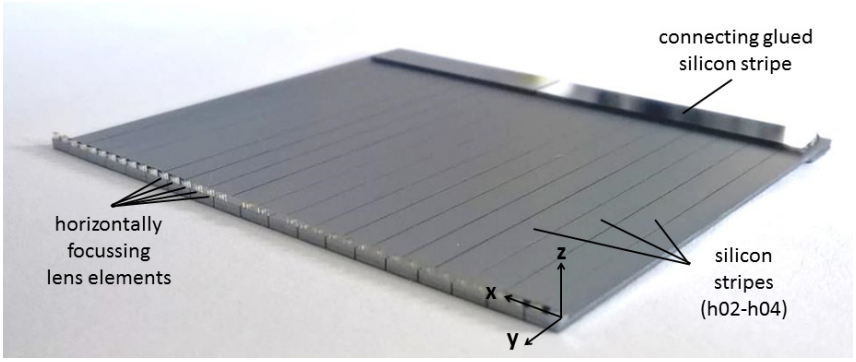

Fig. 6. Line focus CRL row glued on a Si-wafer, cut with a wafer saw to 19 silicon stripes (h01-h19) and connected with a glued silicon stripe at the opposite end.

No positioning errors resulting from the preceding fabrication steps, compared to an uncut lens, along the optical axis (x) and perpendicular to the optical axis and parallel to the substrate (y) could be measured with an optical microscope (NA = 0.95, precision ± 0.3 µm). The prepared half lenses are mounted on the lens alignment setup where they are clamped to the piezo bender actuators. Subsequently, the deadlock for the silicon stripes is adjusted to slightly pre-stress the stripes to ensure the correct alignment of the lens elements in the beam. Therefore, the preload is slightly increased by tightening the deadlock holding screws until all ends of the silicon stripes are in contact with the deadlock bar. This is controlled by measuring the z-positions of the stripe tips with an optical microscope. With a sufficient preload the only factor influencing the accuracy of the lens element positioning is the cylindrical shape of the deadlock. In this setup a 3 mm diameter aluminum bar is used with a measured maximum deviation from linear shape of 4.6 µm along the 60 mm length of the CRL. The short distance of 5 mm between the deadlock bar and the lens elements ensures that a misalignment at the position of the lens elements is not significantly larger than at the position of the deadlock bar. Even so, geometry deviations of the deadlock bar even in the ten micrometer range would not be critical. The stripe length of 45 mm ensures that the line focus lens elements would only be slightly shifted perpendicular to the stripes surface, and that this would not affect the quality of a line focus lens. The tilt angle which would result from even a 50 µm deviation of the deadlock bar from linear would be about 0.1°, which is still in an uncritical range.

The mounting setup of a zoom lens [see Fig. 7] consists of three translational stages (x, y, z) one rotational (rot y) and one tilting stage (rot x, rot z) to align the two half lens holders relative to each other with six degrees of freedom. This adjustment and mounting step ensures that a single well-aligned point focus for the two line focus CRLs is formed. Figure 7 shows the position of the two mounted half lenses with one half rotated by 90° with respect to the other around the optical axis.

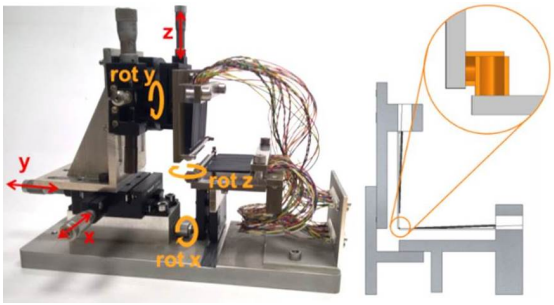

Fig. 7. Mounting setup of a zoom lens with stages of six degrees of freedom (left) and model of a zoom lens with the CRL position (right).

Optics EXPRESS

In order to hold the aligned position, an angle piece made of invar is glued on the backside of the two half lens holders. Lastly, the complete zoom lens is detached from the lens alignment setup and fixed to an adapter for beamline operation [see Fig. 8].

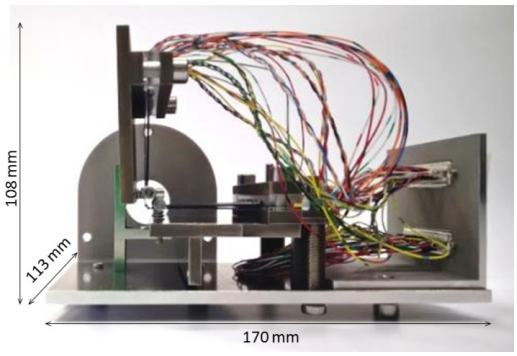

Fig. 8. Complete zoom lens with point focus mounted at an adapter for the ESRF beamline ID01.

4. Electronic controller system

Each piezo bender actuators need a two wire connection for switching. Only two positions are accessible: in and out. One pin is always connected to ground and the other pin can be switched between ground and 200 V [see Fig. 9]. One switching between unbent and bent position in this setup takes about 10 ms considering the charging time of a condenser by approximately $5*\tau$. The time constant τ (in seconds) is given by

$$\tau = RC, \tag{8}$$

where R is the resistance (50 kΩ + 50 kΩ + 1 kΩ) and C is the capacitance (20 nF).

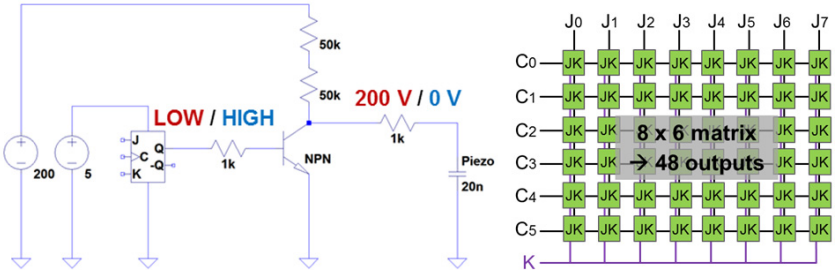

Fig. 9. Logic for one switching channel for a piezo bender actuator with 200 V (left) and channel matrix of JK-flip-flops as an interface between microcontroller and actuators (right).

A microcontroller Arduino Due (Arduino AG) connected via USB to a PC is used to electronically control and conFig. 37 actuators. The digital output signals of the Arduino can be set to either HIGH- or LOW-state. As these outputs only provide 3.3 V as HIGH-signal, a bipolar junction transistor (BJT) circuit is used on an interface [see Fig. 9] to amplify the signal to 200 V for the piezo actuators. The outputs Q of the JK flip-flops are connected to the base of the BJT. If V_{IN} of the transistor is LOW (0 V) it is not conductive and V_{OUT} provides 200 V coming from the designed switched mode power supply (SMPS). Is V_{IN} switched to HIGH (3.3 V) the transistor is conductive and V_{OUT} drops to 0 V.

The number of channels of the Arduino Due is limited therefore the interface is designed with a matrix of JK flip-flops. A flip-flop has two stable states and can be used to store state information. The circuit can change state by signals applied to the three control inputs J (= Set), K (= Reset) and C (= Clock) and will have two outputs Q and $\overline{Q}$. The designed 8x6-

Optics EXPRESS

matrice [see Fig. 9] is capable of changing 48 outputs independently, although only 15 inputs controlled by the microcontroller are needed for the prototype device. The flip-flops are set to HIGH with 8 J-inputs and 6 C-inputs. To reset the flip-flops to LOW, 1 K-input together with all 6 C-inputs are set.

5. Measurement methods and results

This section will present the measurements and results obtained at two different synchrotron beamline setups. At PETRA III-P05 tests were performed with a first zoom lens with the layout described in section 2, showing severe deficits due to mounting errors of the half lenses. Based on the results from this beamline an improved second zoom lens prototype was used at ESRF-ID01.

PETRA III – beamline P05

In this experiment two half lenses were tested separately at an energy of E = 18.4 keV to obtain line foci. For a number of zoom lens combinations the image distance d_i and focal spot size σ were measured by detector scans along the optical axis around the focal plane. The image distance d_i was measured from the focal plane to the first lens element h01/v01 counted from the source side. The focal spot size was calculated using the variance of the intensity plot in the focal plane. A Gaussian function was fitted to the measured values which were all obtained at an energy of E = 18.4 keV. The measured focal spot sizes σ_m were in the range of 6 - 8 µm, much larger than the diffraction limit ($\sigma_{min.diff}$ = 0.37 µm) of a complete lens of 36 elements with the same layout with f = 357 mm. Additionally, considering the source width of 100 µm at 65 m source distance and 2.1 m image distance, the geometric image of the source is 3.7 µm. Table 1 compares the measured optical properties of this CRL (layout 1405_00_A0, #10) with calculated values.

Table 1. Results of the optical properties of CRL layout 1405_00_A0, #10 at PETRA III, P05 at 18.4 keV.

Silicon stripes in the beam	Number of lens elements N	Calculated image distance $d_{i,c}$	Measured image distance $d_{i,m}$	Calculated focal spot size σ_c	Measured focal spot size σ_m
h05-h07	6	2081 mm	2180 mm	3.31 µm	7.91µm
h01-h02 + h07	6	2084 mm	2195 mm	3.42 µm	8.46 µm
h01-h03 + h07	8	1564 mm	1612 mm	2.44 µm	7.36 µm
h05-h08	8	1562 mm	1620 mm	2.44 µm	7.69 µm
h04-h08	10	1250 mm	1280 mm	1.96 µm	7.54 µm
v05-v09	10	1251 mm	1270 mm	1.96 µm	6.07 µm

The focal sizes are two to three times larger than the expected ones. This is due to imprecise positioning of the half lenses caused by deficits in construction and fabrication. These results gave us valuable hints for further investigating and optimizing the fabrication steps of a zoom lens.

ESRF – beamline ID01

After optimization of both the zoom lens setup and the assembly procedure, a second test was performed at ESRF beamline ID01. The first complete zoom lens for point focusing was analyzed at two energies, 10 keV and 19.5 keV. To prove the concept and test the quality of the lens five different zoom lens configurations M1-M5 were evaluated at 10 keV and configurations M1-M2 again at 19.5 keV. At ID01 a Basler camera with 3.75 µm x 3.75 µm pixel size was used to align the zoom lens in the optical path [see Fig. 10].

Optics EXPRESS

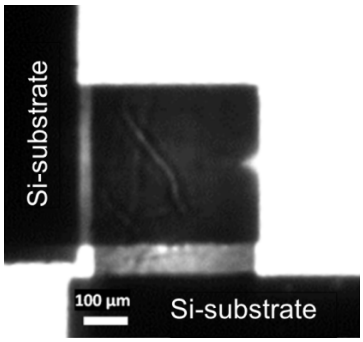

Fig. 10. Alignment of the point focus zoom lens at ESRF ID01 at E = 10 keV.

The quality of the zoom lens was evaluated with a knife-edge measurement [see Fig. 11]. A 250 µm diameter electrical discharge machining wire served as the blade. The image distance in this measurement is defined from the center of the lens to the focal plane.

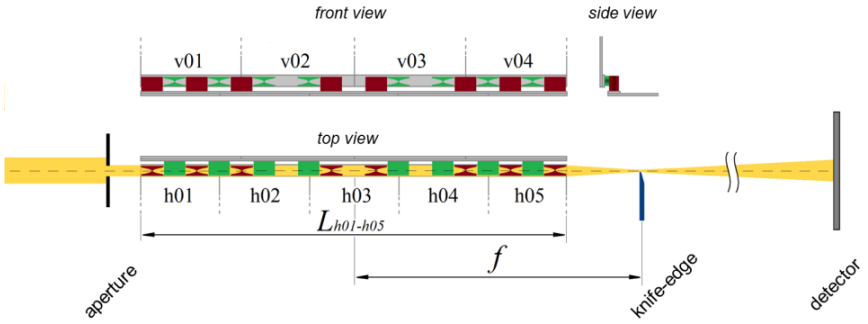

Fig. 11. Simplified schematics of an X-ray zoom lens with point focus measured with knife-edge scan.

In Table 2 the calculated image distances and focal spot sizes are compared to the measured values. The image distances are all in the expected range. Differences between the calculated [Table 2, col. 4] and measured [Table 2, col. 5, 6] distances are within the measurement precision which is ± 5 mm. This verifies the concept and functionality of the zoom lens. Focal spot sizes in the range of σ = 0.45 µm to 1.37 µm were obtained [see Fig. 12 and Table 2, col. 9, 11].

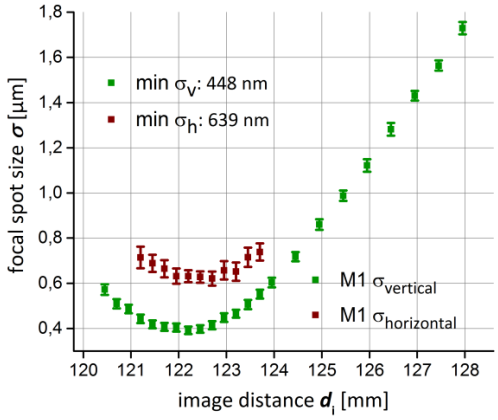

Fig. 12. Measurement of image distance and of the focal spot size in vertical and horizontal direction in configuration M1 at E = 10 keV.

Optics EXPRESS

The setup of configuration M1 at E = 10 keV can achieve a focal spot size of 0.35 µm representing the diffraction limit [see Table 2, col. 7]. When the source size of 15 µm x 135 µm (vertical x horizontal) in 120 m distance and 126 mm image distance as well as the astigmatism (see section 2) is also considered the minimal focal spot size $\sigma_{\text{min. total}}$ is 0.45 µm x 0.64 µm (vertical x horizontal) [see Table 2, col. 8, 10]. Here the geometrical mean for all three σ (5)-(7) is used as a good approximation of the minimum total focal spot size $\sigma_{\text{min. total}}$. Compared to the minimal achievable focal spot sizes the measured focal spot sizes are larger by a factor of 1.2 to 3.3. In fixed focus CRLs of the same type, such high deviations do not occur.

Table 2. Results of first measurements of a point focus zoom lens at ESRF, ID01 with simulated image distance and calculated focal spot sizes compared to measured values in five configurations at 10 keV and 19.5 keV.

Photon energy	Configuration	Number of lens elements	Calculated image distance	Measured vertical image distance	Measured horizontal image distance	Min. diffraction limited focal spot size	Min. focal spot size with real vertical source size incl. astigmatism	Measured vertical focal spot size	Min. focal spot size with real horizontal source size incl. astigmatism	Measured horizontal focal spot size
10 keV	M1	3 2	126 mm	122 mm	122 mm	0.35 µm	0.42 µm	0.45 µm	0.44 µm	0.64 µm
	M2	2 8	141 mm	142 mm	143 mm	0.32 µm	0.39 µm	0.54 µm	0.42 µm	1.14 µm
	M3	2 8	142 mm	143 mm	144 mm	0.27 µm	0.38 µm	0.89 µm	0.41 µm	1.37 µm
	M4	2 4	162 mm	162 mm	166 mm	0.31 µm	0.39 µm	0.60 µm	0.43 µm	0.67 µm
	M5	2 4	164 mm	165 mm	167 mm	0.31 µm	0.39 µm	0.60 µm	0.43 µm	0.60 µm
19.5 keV	M1	3 2	453 mm	448 mm	448 mm	0.21 µm	0.28 µm	0.79 µm	0.58 µm	1.18 µm
	M2	2 8	510 mm	514 mm	516 mm	0.21 µm	0.29 µm	0.92 µm	0.64 µm	1.27 µm

As can be seen from the values in the table, there is a strong difference for the deviations in the measurements of horizontal and vertical image distances and focal spot sizes. Astigmatism due to half lenses layout difference as described in section 2 is one reason. Additionally, the two CRL halves are mounted slightly asymmetrically [see Fig. 10]. The horizontally focusing lens elements were slightly rotated by 0.07° around an axis perpendicular to their substrate. One more reason for the deviations could be that the real source size of the beamline might have been larger than expected. This need to be investigated in future experiments.

6. Conclusion

A point focus X-ray zoom lens has been realized and characterized at ID01, ESRF after first line focus tests at P05, PETRA III and following necessary construction and process improvements. The zoom lens has a compact size with an overall volume of two liters. The concept uses bending piezo actuators to reversibly move CRL elements in and out of the beam. The lens elements are placed on silicon stripes. It allows the focal length to be changed within 10 ms and thus is perfectly suited for setups requiring very fast reconfiguration. The system includes a 200 V-piezo controller and is remote controlled via USB. As horizontal and vertical focal lengths can be chosen separately and the position of lens elements can be configured freely, the optics can be virtually free of astigmatism, independent of the chosen photon energy. At beam lines with a more line shaped source, astigmatism can be introduced deliberately to get a more round focal spot at the sample.

Optics EXPRESS

The CRL used in the actual zoom lens provides focal lengths from about 77 mm to 46 m at photon energies of 8 - 50 keV. The transmission in this range is between 3% for 8 keV and 47% for 50 keV. It was shown that the calculated focal length was achieved in the measurements for five lens configurations at two energies. The optical characterization has proven a minimum spot size of 0.45 µm which is only 7% larger than the expected theoretical value. In average the measured values were about a factor of two larger than the calculated value.

Future versions of the zoom lens will provide LAN-connection and software to automatically choose the optimum combination of lens elements for a requested photon energy, source and sample distance. These lenses could beneficially be used in all applications, where changing photon energies requires a flexible and fast adaptation of the optics, like full field microscopy or spectroscopy. In other applications the systems small footprint could be advantageous. The concept could be also adapted directly to interdigitated silicon or diamond lenses.

Funding

Karlsruhe School of Optics and Photonics (KSOP).

Acknowledgments

The authors thank the ESRF for providing beam time at ID01 as well as Helmholtz-Zentrum Geesthacht and DESY for providing beam time at PETRA III beamline P05. We thank the Karlsruhe Nano Micro Facility (KNMF), a research infrastructure in the Helmholtz association for the possibility to fabricate the polymer X-ray lenses by X-ray lithography. We further acknowledge the support of the Karlsruhe School of Optics and Photonics (KSOP).